

3D Face Reconstruction by Learning from Synthetic Data

Elad Richardson* Matan Sela*

Ron Kimmel

Technion - Israel Institute of Technology

{eladrich, matansel, ron}@cs.technion.ac.il

Abstract

Fast and robust three-dimensional reconstruction of facial geometric structure from a single image is a challenging task with numerous applications. Here, we introduce a learning-based approach for reconstructing a three-dimensional face from a single image. Recent face recovery methods rely on accurate localization of key characteristic points. In contrast, the proposed approach is based on a Convolutional-Neural-Network (CNN) which extracts the face geometry directly from its image. Although such deep architectures outperform other models in complex computer vision problems, training them properly requires a large dataset of annotated examples. In the case of three-dimensional faces, currently, there are no large volume data sets, while acquiring such big-data is a tedious task. As an alternative, we propose to generate random, yet nearly photo-realistic, facial images for which the geometric form is known. The suggested model successfully recovers facial shapes from real images, even for faces with extreme expressions and under various lighting conditions.

1. Introduction

Extracting the geometry of a surface embedded in an image is one of the fundamental challenges in the field of computer vision. Generally speaking, the problem is ill-posed as different textured surfaces can be realized as the same image on a camera sensor. Hence, when dealing with a certain class of shapes, it is common to employ prior knowledge for simplifying the problem. In fact, reconstruction methods often differ in the way they utilize prior knowledge.

The unique challenge in face reconstruction is that although faces are, roughly speaking, very similar, there are local discrepancies between faces of different people. Capturing these local differences is crucial for accurate facial



Figure 1: Reconstruction samples from our network. From left to right: a given facial image, a shading image of the reconstructed geometry representation predicted by our network, a textured reconstruction shown from a different viewing angle and under different lighting conditions.

geometry reconstruction. A common approach for recovering face geometries is to apply an optimization procedure in which both geometry and lighting conditions are iteratively updated to best match the given image. As an example, the analysis-by-synthesis approach introduced in [3] alternates between rendering the reconstructed face and updating the representation and illumination parameters. There, the prior comes in the form of the solution space, which is represented by a linear regression model built from a few hundred scans of facial geometries. Although this approach can achieve highly accurate results, it requires manual initialization and focuses on faces with natural expressions.

Alternatively, recent methods [1, 10, 17] use a sparse set of 2D landmarks to directly infer the face geometry. The usage of landmarks makes these algorithms more robust to lighting and albedo changes, as they are not directly dependent on the image. However, these algorithms strongly depend on the landmark detection accuracy and cannot recover fine details which are not spanned by the sparse set of landmarks. Here, we propose to train a neural network for directly reconstructing the geometric structure of a face embedded in a given image. The benefits of using a neural network in this context are clear. First, a network reconstructs the geometry based on the image as a whole. Second, it can implicitly model different rendering methods, and third, it can be incorporated into real-time face reconstruction systems.

Convolutional neural networks have recently revolutionized computer vision research and applications with promising performance when applied to image classification and regression problems. However, thousands of annotated samples are usually required for training a network which generalizes well. In the case of three-dimensional faces, no suitable large dataset is currently available. To that end, we propose to train our network with synthetic ex-

*Equal contribution

amples of photo-realistic facial images. The faces we randomly draw from our model vary extensively in their pose, expression, race and gender. Moreover, the images we synthesize have different illumination conditions, reflectance and background. The proposed synthetic dataset construction allows us to introduce a computational model that can handle real images of faces in the wild. That is, by training with artificial data that we synthesize, we can reconstruct surfaces of faces from natural images.

Our main contributions are as follows:

- We introduce a novel method for generating a dataset of nearly photo-realistic facial images with known geometries.
- For the first time, a network is successfully trained to recover facial geometries from a single given image, based on synthetic examples.
- We exploit the fact that the space of facial textures and geometries can be captured by a low dimensional linear space. It is used in synthesizing the images and their corresponding geometries, and then in the reconstruction phase, where the output is a small number of coefficients in that space.

2. Related Efforts

Various approaches have been proposed for tackling the inherently ill-posed problem of facial geometry reconstruction from a single image. In [3], Vetter and Blanz observed that both the geometric structure and the texture of human faces can be approximated as a linear combination of carefully designed vectors. For constructing this linear model, dubbed as the 3D Morphable Model (3DMM), they scanned a few hundred subjects, found a dense registration between them, and applied a principal component analysis on the corresponding scans. For computing a plausible representation of a face in a given image, Vetter and Blanz proposed an analysis-by-synthesis approach which alternates between rendering a reconstruction and refining the geometry, texture, and illumination parameters according to the differences between the given image and the rendered one.

Alternatively, in [14], Kemelmacher-Shlizerman and Basri proposed to recover the geometry using a shape from shading approach, where a single 3D reference face is manually placed in alignment with a given input facial image in order to constrain the problem. A low-dimensional representation of reflectance based on spherical harmonics [2] is assumed, and the lighting coefficients are recovered based on the normals and albedo of the aligned reference face. Then, the depth image and the albedo of the face are recovered based on the difference between the input image and the reconstructed one, generated with the recovered illumination parameters. Note that both this method and the

previous one explicitly employ the image acquisition model as part of their optimization and rely on an accurate initialization.

As landmark detection algorithms have become faster and robust [13, 21, 25, 26] it is now common to use them for facial reconstruction. Some methods use these detection algorithms to automate the reconstruction process of existing methods. As an example, in [5], feature points are used for rigidly aligning a 3D face model with the image. The 3D face is then refined by deploying the method of Vetter and Blanz [3]. Still, automated initialization usually does not produce the same level of accuracy as manual ones, as shown in [20]. Other methods [1, 10, 17] choose to reconstruct the geometry solely from the detected landmarks. These methods allow fast reconstructions and are usually more robust to lighting and albedo variations. However, landmarks still incorporate only sparse information about the geometrical structure of the face, thus limiting the quality of the results. This is sufficient for some tasks, such as in [28], while other require further refinement as applied in [22] for facial reconstruction from multiple images.

Recently, the 3DMM model was integrated with convolutional neural networks [12, 27] for recovering pose variations of faces in images. The networks were trained by augmentations of existing datasets of face alignment challenges. These approaches suggest that given a suitable dataset, a CNN can successfully recover the morphable model coefficients from an image.

Training a network with synthetic data for shape recovery purposes was also suggested by Li *et al.* in [16]. There, a network was trained for extracting joint embedding of images and their corresponding 3D rigid objects. The synthetic images were generated from the manually collected ShapeNet dataset [7]. The ShapeNet dataset was also recently used for the 3D object reconstruction method in [8]. Here, we extend the concept of training from synthetic data by automatically generating a large dataset of facial images labeled with corresponding 3DMM representations.

3. Overview

An example of the proposed pipeline for recovering facial geometry from a single given image is visualized in Figure 2. First, the input image is masked according to the projection of a generic 3D facial model on the image. The facial model is posed using the automatic alignment algorithm from [13]. The masked image is then propagated multiple times through the network, iteratively updating the geometry representation. This network is trained on synthetic images of textured three-dimensional faces as shown in Section 6. These images are rendered from geometric and photometric structures drawn from the 3DMM model as described in Section 4. The network architecture and training method is detailed in Section 5. Finally, as an optional step,

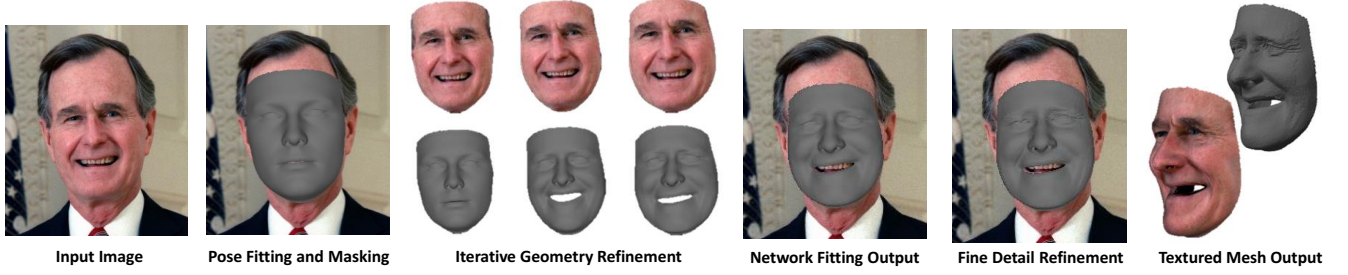


Figure 2: The pipeline of the proposed algorithm. The method starts with an arbitrary facial image and returns a detailed geometric facial reconstruction.

we demonstrate how the resulting facial structure can be further refined by a shape from shading algorithm in Section 7.

4. The Face Model

In order to model different plausible geometries, the 3D Morphable Model is used. As in the framework proposed by Chu *et al.* in [9], the representation is decomposed into identity and expression bases. The identity basis A_{id} is a compact principal component basis introduced in [3] and the expression basis A_{exp} is a set of blendshapes, where each vector represents an offset from neutral facial identity to a specific expression. The geometry of a given subject is linearly represented as

$$S = \mu_S + A_{id}\alpha_{id} + A_{exp}\alpha_{exp}. \quad (1)$$

Here, μ_S denotes the average shape. α_{id} and α_{exp} are the corresponding coefficient vectors of identity and expression, respectively. As the proposed model is obviously restricted to geometries and expressions spanned by the proposed basis, examples need to be collected with care. We used the reconstructions from the Bosphorus dataset [23], augmented with some in-house data, and aligned using a non-rigid ICP [24] procedure. For spanning neutral geometric facial structures, we construct an identity basis with 200 vector elements, augmented by 84 vectors of various expressions.

The 3DMM model also represents the texture of the face as a linear combination of vectors. This model is constructed similarly to the model of identity geometries by computing the principal components basis of the registered scanned faces. Each texture is then represented as

$$T = \mu_T + A_T\alpha_T, \quad (2)$$

where μ_T is the average texture, A_T is the texture basis and α_T is the coefficients vector. For the texture model, we used 200 basis elements. In practice, using a significantly smaller number of basis elements for both geometry and texture produces comparable results.

5. Learning Framework

At the center of our pipeline lies the network, which predicts the face geometry from the image. Next, we describe how this network operates.

5.1. Iterative Formulation

In its basic formulation a Convolutional-Neural-Network (CNN) is a feed-forward system, predicting the outputs from the inputs in a single pass. However, the power of one-shot algorithms is somewhat limited, as unlike iterative algorithms they cannot correct wrong predictions. Inspired by [6], we run our network iteratively. The core idea of iterative error feedback (IEF) is to use a secondary input channel to represent the previous network’s output as an image. The network can then be trained to correct the previous prediction based on both the original input and the secondary channel. Representing the geometry coefficients as an image can be done in several different ways. Here, we choose to represent it as a shading image from a frontal light source, where the geometry is aligned using an initial pose derived using [13]. The IEF architecture is presented in Figure 3, alongside an example of the input channel. Note that un-

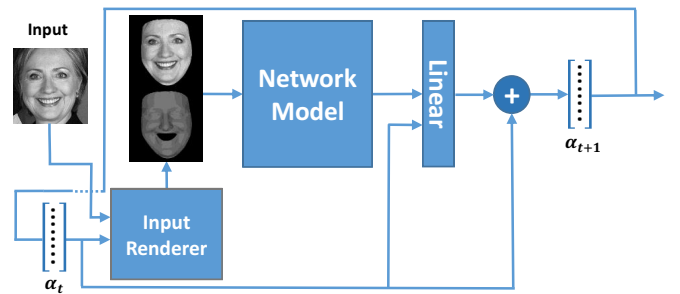


Figure 3: Iterative architecture. In every iteration inputs are generated based on the the previous prediction and propagated through the network. A linear layer then determines the geometry coefficient update.

like [6] we also add a linear layer which takes as input both the current network’s output and the previous prediction, producing the actual correction.

During evaluation, we initialize the geometry using the average shape, setting $\alpha_0 = 0$. This geometry is then used to create the shading image, as well as to mask the input image from the background. At every iteration, a new geometry vector, α_t , is predicted and used to update the shading image and the masking of the input image. The procedure repeats ~ 3 times improving the masking and the reconstruction iteratively. The purpose of masking the face in the input image is to simplify the data generation process. That way we only need to accurately synthesize the face itself.

5.2. Training Criterion

An important choice for the learning framework is the loss criterion. A trivial choice in our case would be to use Mean Square Error (MSE) between the output representation vector and the ground-truth vector. However, that formulation does not take into account how the different coefficients affect the geometry. Instead, the criterion is defined as the MSE between the geometries themselves:

$$L(x, y) = \|[A_{\text{id}}|A_{\text{exp}}]x - [A_{\text{id}}|A_{\text{exp}}]y\|_2^2, \quad (3)$$

where x is the output of the network, and y is the known geometry. As this loss is differentiable it can be easily incorporated into the training procedure. Note that all geometries are aligned, which justifies measuring error between corresponding vertices. Using this geometry MSE allows the network to take into account how changes in the coefficients would affect the final reconstruction error, and results in better convergence.

5.3. Network Architecture

The proposed network architecture is based on ResNet [11], winner of the ILSVRC 2015 classification task. The architecture is detailed in Figure 4, where the input is of size 200x200x2. The additional linear layer men-

layer	stride	output size
7x7, 32	2	100x100x32
b[32] x 2	1	100x100x32
b[64] x 2	2	50x50x64
b[128] x 2	2	25x25x128
b[256] x 2	2	13x13x256
3x3, 284	1	13x13x284
averaging	-	284

Figure 4: Network architecture. b[n] denotes a building block, as in the ImageNet architecture of [11], with n output maps. Padding is used in all layers.

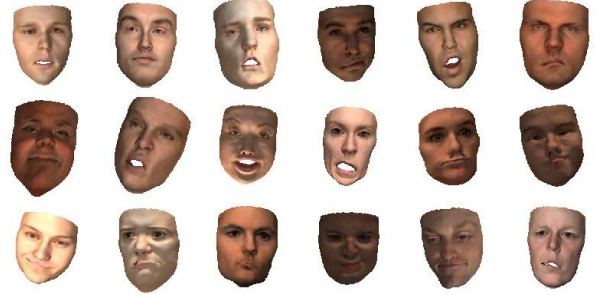


Figure 5: Samples of the synthetic images generated by the proposed model.

tioned in Section 5.1 has an input of size 568, and an output of size 284. The network was optimized using the ADAM method [15] with a fixed learning rate.

6. Data Generation

An essential part of every learning algorithm is the training dataset. Without a good training set of sufficient size, the learning model would simply fail to characterize the data. For CNNs, where models with millions of parameters are commonly used, the generalization problem becomes even more complex, and one must often rely on large scale datasets to train a model. However, existing datasets of 3D faces usually consist of just a few hundreds of subjects, making them unsuitable for deep learning tasks. Ideally, one could capture enough 3D faces and use them to train a CNN model similarly to the suggested method. However, scanning millions of faces with an accurate depth sensor is currently impractical. Alternatively, one could take a set of 2D images and apply a reconstruction algorithm to generate the geometric representation. Still, such an approach would limit our reconstruction capability to that of the specific geometry reconstruction algorithm we use, and, in practice, we will merely learn the potential shortcomings of that algorithm. Instead, we propose to directly generate different geometries using a morphable model. Each such geometry is then rendered under random lighting conditions and projected onto the image plane. This gives us a set of images for which the ground truth geometry is known. In practice, generating a 3D face using 3DMM requires drawing a random normally distributed coefficients vector for the model described in Section 4.

6.1. Rendering The Geometries

Given a textured 3D geometry, a synthetic image can be rendered. First, random shading needs to be drawn to create photo-realistic results. We use Phong reflectance [19] for modeling the shading. In our formulation the shininess constant was fixed at 10, while the ambient, diffuse and specular constants were normally drawn around mean val-

ues of $[0.5, 0.7, 0.05]$ respectively. The light direction was drawn from a uniform distribution, covering all possible frontal angles.

The shaded geometry is then projected onto the image plane, with a parallel weak perspective projection, as

$$\begin{bmatrix} p_x \\ p_y \end{bmatrix} = \begin{bmatrix} f & 0 & 0 \\ 0 & f & 0 \end{bmatrix} [R|t] \begin{bmatrix} P_x \\ P_y \\ P_z \\ 1 \end{bmatrix}. \quad (4)$$

Rotation, translation and scaling parameters are all normally sampled and the mean value is set to form a front-facing centered face. Geometries sampled from the proposed model are shown in Figure 5.

6.2. Iterative Data Simulation

The network operates in an iterative error feedback fashion, as detailed in Section 5.1. This means that during evaluation the network always receives two inputs. The first one being the cropped input image, while the second one is the shading image, representing the current geometry estimation. The network then predicts a correction to the geometry estimation. For training our network, a dataset of such samples needs to be generated. That is, each dataset sample needs to include a cropped input image, some geometry estimation, and the ground-truth geometry as a label.

The actual generation is done as follows. First, we generate a random 3D face by drawing a ground-truth geometry, α_{gt} , and a texture. The 3D face is then rendered as explained in the previous section. We then proceed by drawing another geometry, α_t , as our current geometry estimation. α_t is then used to generate the shading image and to mask the rendered facial image. See Figure 6 for generation examples. Note that the same projection is used for both geometries. The sampling of α_t needs to simulate the process of refining the initial geometry towards the real one. This

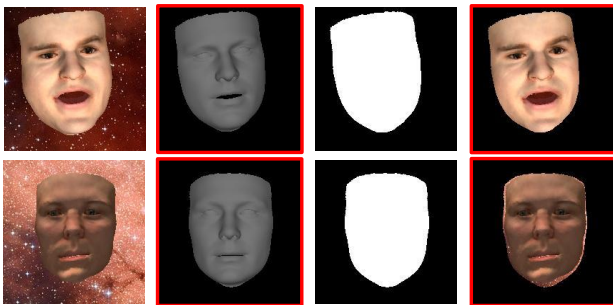


Figure 6: Training data sample generation. From left to right: Generated facial image. Generated secondary geometry rendered as a shading image. Binary mask of the shading image. Cropped facial image. The training pairs of the network are the images marked in red.



Figure 7: Shape from shading refinement. From left to right: the input image, the network-based reconstruction, and the same reconstruction after shape from shading.

is being achieved by uniformly sampling it between some random geometry and α_{gt} . That way, our dataset includes samples in various distances from α_{gt} .

7. Extracting Fine Details

One of the limitations of using 3DMM to model the space of plausible geometries is that the results are constrained to the affine subspace spanned by the 3DMM vectors. Consequently, 3DMM cannot model fine details such as the wrinkles around the eyes. To solve this, we employ the real-time shape-from-shading (SFS) algorithm of Or-El *et al.* [18]. The predicted geometry is used as input to the algorithm, which then refines the reconstruction. Note that the predicted geometry needs to be accurate at a coarse scale for the SFS refinement to work. Experiments show that this formulation can successfully reconstruct fine details when used as a post-processing step.

8. Results

To show the generalization capability of our method we evaluate it on image of real faces *in-the-wild*. For a visual analysis of the reconstructions, we recover the texture according to the image and render the colored face from different viewing direction and under various lighting conditions. Note, that some regions of the face are naturally occluded. This prohibits a full recovery of the texture. In order to fill these gaps, we first project the recovered texture onto the linear texture model, and set the missing values according to the reconstructed texture. The texturing process is visualized in Figure 8.



Figure 8: Texturing process. From left to right: The initial texture with missing values derived from the image, the texture retrieved from the linear model, and the combined one which is used for presenting the results in this paper.

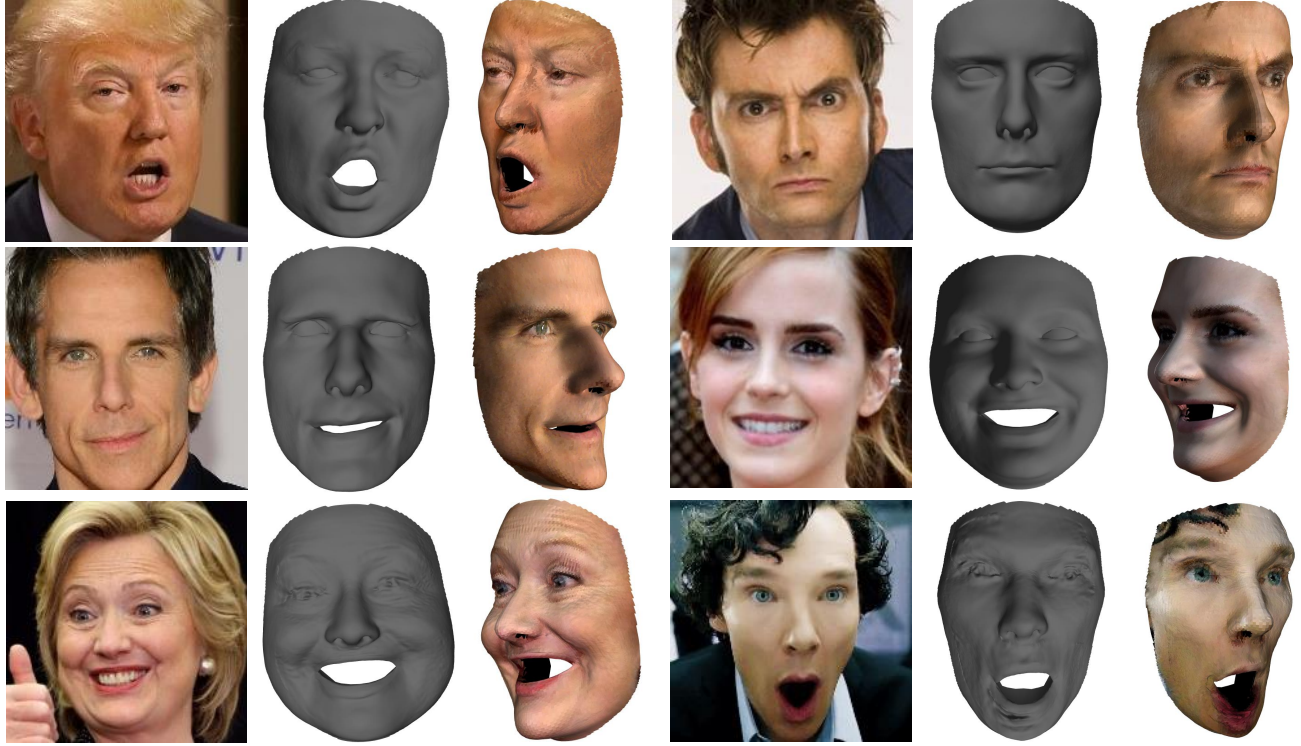


Figure 9: Results of the proposed algorithm. The first two rows visualize reconstructions without a shape from shading phase, while the last row presents results with the refinement step.

Different results of the proposed method are shown in Figures 1 and 9. As demonstrated, the method successfully reconstructs *in-the-wild* faces under different illumination conditions, viewpoints and expressions. The effect of the SFS phase can be scrutinized in Figure 7, where zoomed-in images of the reconstructions are shown.

As mentioned in Section 2, landmark detection algorithms are utilized by different methods for 3D face reconstruction. One common technique is to estimate a set of 3DMM parameters by minimizing the L_2 difference between the 2D image landmarks and the projected 3DMM landmarks. In Figure 10 we compare the reconstruction achieved directly based on 68 image landmarks to the one generated by the proposed network. As demonstrated, the proposed method successfully reconstructs more details, such as the shape of the nose and the wrinkles around the mouth, which are not spanned by the sparse set of landmarks.

A quantitative comparison between the proposed method and a landmark based reconstruction is given in Figure 11. For evaluating the accuracy of the reconstruction we registered our average shape to several 3D scans from the FRGC-v2.0 dataset using a non-rigid registration, and used the warped template as our ground truth. Then, we aligned each

reconstruction with the ground truth by the optimal similarity transform, and computed the pointwise Euclidean distance between corresponding points on the two shapes. As demonstrated, in these cases, the network recovers the subtle details of the face more accurately.



Figure 10: Method Comparisons (without SFS). The first row shows the input image. The second row shows reconstruction based only on landmark points. The third row shows the reconstruction results of the proposed methods.



Figure 11: Quantitative analysis of the proposed method vs. landmark point based reconstruction. Each face is colored according to the pointwise Euclidean error (in millimeters) of the reconstruction.

9. Discussion

The proposed approach was shown to recover relatively accurate facial geometry from a single image. In our experiments, we explored other alternative configurations. For example, we compared the usage of full-perspective projections versus weak perspective ones. According to our findings, the latter outperformed the former. We believe that the superiority of the weak perspective projection can be explained by the ambiguity in initializing the face mask parameters under a full-perspective projection. That is, a narrow face may correspond to either a round geometry close to the camera or a narrow one viewed from a distance.

There are numerous possible options for extending the proposed method. For example, as the suggested network does not require explicit representation of the rendering model, more accurate rendering techniques can be easily incorporated to create more realistic synthetic images without changing the learning framework. One such option is to use a ray casting shader which imitates more precisely the image acquisition process. Intuitively, the more similar the synthetic data is to real *in-the-wild* images the better the network’s result should be. Another possible direction is to incorporate face landmarks as another input into the suggested algorithm, utilizing the robustness of landmark detection. Finally, as all components of the suggested pipeline can be implemented to run in real-time on a GPU, the proposed method can possibly be used for real-time face reconstruction from video. The iterative formulation of the network would allow us to solve every frame based on the previous one without modifying the architecture.

9.1. Limitations

Although, in many cases, the suggested algorithm performs well, we encountered some scenarios which prohibited the network from recovering the geometry. Firstly,

since the 3DMM model was constructed by scanning faces from specific ethnic origins, the proposed approach sometimes fails to fully recover images of faces which are not spanned by the scanned faces. Secondly, we found that the network occasionally makes mistakes when faced with facial attributes which were not present in the synthetic data. For example, thick lips with lipstick could be mistaken for the interior of the mouth, while beards could be mistaken for parts of the background, as shown in Figure 12. Both problems can be solved by incorporating a richer model such as the one proposed in [4] and using better, and more accurate, rendering techniques.



Figure 12: Limitations of the reconstruction.

10. Conclusion

We proposed an efficient algorithm for recovering facial geometries from a single image. The proposed approach reconstructs the face based on the image as a whole. For this, we employ an iterative Convolutional-Neural-Network trained with synthetic data. As an optional detail refinement step, a shape-from-shading algorithm was applied. We evaluated the method by recovering facial surfaces from various pictures of faces *in-the-wild*. As demonstrated, the proposed approach successfully generalizes from our synthetic data and can efficiently and accurately handle a large variety of expressions and different illumination conditions.

Acknowledgments

The research leading to these results has received funding from the European Research Council under European Unions Seventh Framework Programme, ERC Grant agreement no. 267414. The authors would like to thank Mr. Roy Or-El for providing the source code of the shape from shading algorithm.

References

- [1] O. Aldrian and W. A. Smith. A linear approach of 3d face shape and texture recovery using a 3d morphable model. In *Proceedings of the British Machine Vision Conference*, pages 75–1, 2010. 1, 2
- [2] R. Basri and D. W. Jacobs. Lambertian reflectance and linear subspaces. *IEEE Transactions on Pattern Analysis and Machine Intelligence*, 25(2):218–233, Feb 2003. 2
- [3] V. Blanz and T. Vetter. A morphable model for the synthesis of 3d faces. In *Proceedings of the 26th annual conference on*

- Computer graphics and interactive techniques*, pages 187–194. ACM Press/Addison-Wesley Publishing Co., 1999. 1, 2, 3
- [4] J. Booth, A. Roussos, S. Zafeiriou, A. Ponniah, and D. Dunaway. A 3d morphable model learnt from 10,000 faces. 7
 - [5] P. Breuer, K.-I. Kim, W. Kienzle, B. Scholkopf, and V. Blanz. Automatic 3d face reconstruction from single images or video. In *Automatic Face & Gesture Recognition, 2008. FG'08. 8th IEEE International Conference on*, pages 1–8. IEEE, 2008. 2
 - [6] J. Carreira, P. Agrawal, K. Fragkiadaki, and J. Malik. Human pose estimation with iterative error feedback. In *The IEEE Conference on Computer Vision and Pattern Recognition (CVPR)*, June 2016. 3, 4
 - [7] A. X. Chang, T. Funkhouser, L. Guibas, P. Hanrahan, Q. Huang, Z. Li, S. Savarese, M. Savva, S. Song, H. Su, et al. Shapenet: An information-rich 3d model repository. *arXiv preprint arXiv:1512.03012*, 2015. 2
 - [8] C. B. Choy, D. Xu, J. Gwak, K. Chen, and S. Savarese. 3d-r2n2: A unified approach for single and multi-view 3d object reconstruction. *arXiv preprint arXiv:1604.00449*, 2016. 2
 - [9] B. Chu, S. Romdhani, and L. Chen. 3d-aided face recognition robust to expression and pose variations. In *2014 IEEE Conference on Computer Vision and Pattern Recognition*, pages 1907–1914. IEEE, 2014. 3
 - [10] P. Dou, Y. Wu, S. K. Shah, and I. A. Kakadiaris. Robust 3d face shape reconstruction from single images via two-fold coupled structure learning. In *Proc. British Machine Vision Conference*, pages 1–13, 2014. 1, 2
 - [11] K. He, X. Zhang, S. Ren, and J. Sun. Deep residual learning for image recognition. In *The IEEE Conference on Computer Vision and Pattern Recognition (CVPR)*, June 2016. 4
 - [12] A. Jourabloo and X. Liu. Large-pose face alignment via cnn-based dense 3d model fitting. In *The IEEE Conference on Computer Vision and Pattern Recognition (CVPR)*, June 2016. 2
 - [13] V. Kazemi and J. Sullivan. One millisecond face alignment with an ensemble of regression trees. In *Proceedings of the IEEE Conference on Computer Vision and Pattern Recognition*, pages 1867–1874, 2014. 2, 3
 - [14] I. Kemelmacher-Shlizerman and R. Basri. 3d face reconstruction from a single image using a single reference face shape. *IEEE Transactions on Pattern Analysis and Machine Intelligence*, 33(2):394–405, 2011. 2
 - [15] D. Kingma and J. Ba. Adam: A method for stochastic optimization. *arXiv preprint arXiv:1412.6980*, 2014. 4
 - [16] Y. Li, H. Su, C. R. Qi, N. Fish, D. Cohen-Or, and L. J. Guibas. Joint embeddings of shapes and images via cnn image purification. *ACM Trans. Graph*, 5, 2015. 2
 - [17] F. Liu, D. Zeng, J. Li, and Q. Zhao. Cascaded regressor based 3d face reconstruction from a single arbitrary view image. *arXiv preprint arXiv:1509.06161*, 2015. 1, 2
 - [18] R. Or-El, G. Rosman, A. Wetzler, R. Kimmel, and A. M. Bruckstein. Rgb-d-fusion: Real-time high precision depth recovery. In *Proceedings of the IEEE Conference on Computer Vision and Pattern Recognition*, pages 5407–5416, 2015. 5
 - [19] B. T. Phong. Illumination for computer generated pictures. *Communications of the ACM*, 18(6):311–317, 1975. 4
 - [20] M. Piotraschke and V. Blanz. Automated 3d face reconstruction from multiple images using quality measures. In *Proceedings of the IEEE Conference on Computer Vision and Pattern Recognition*, pages 3418–3427, 2016. 2
 - [21] S. Ren, X. Cao, Y. Wei, and J. Sun. Face alignment at 3000 fps via regressing local binary features. In *Proceedings of the IEEE Conference on Computer Vision and Pattern Recognition*, pages 1685–1692, 2014. 2
 - [22] J. Roth, Y. Tong, and X. Liu. Adaptive 3d face reconstruction from unconstrained photo collections. *CVPR*, 2016. 2
 - [23] A. Savran, N. Alyüz, H. Dibeklioglu, O. Çeliktutan, B. Gökberk, B. Sankur, and L. Akarun. Bosphorus database for 3d face analysis. In *European Workshop on Biometrics and Identity Management*, pages 47–56. Springer, 2008. 3
 - [24] T. Weise, H. Li, L. Van Gool, and M. Pauly. Face/off: Live facial puppetry. In *Proceedings of the 2009 ACM SIGGRAPH/Eurographics Symposium on Computer Animation, SCA '09*, pages 7–16, New York, NY, USA, 2009. ACM. 3
 - [25] Z. Zhang, P. Luo, C. C. Loy, and X. Tang. Facial landmark detection by deep multi-task learning. In *European Conference on Computer Vision*, pages 94–108. Springer, 2014. 2
 - [26] E. Zhou, H. Fan, Z. Cao, Y. Jiang, and Q. Yin. Extensive facial landmark localization with coarse-to-fine convolutional network cascade. In *Proceedings of the IEEE International Conference on Computer Vision Workshops*, pages 386–391, 2013. 2
 - [27] X. Zhu, Z. Lei, X. Liu, H. Shi, and S. Z. Li. Face alignment across large poses: A 3d solution. In *The IEEE Conference on Computer Vision and Pattern Recognition (CVPR)*, June 2016. 2
 - [28] X. Zhu, Z. Lei, J. Yan, D. Yi, and S. Z. Li. High-fidelity pose and expression normalization for face recognition in the wild. In *Proceedings of the IEEE Conference on Computer Vision and Pattern Recognition*, pages 787–796, 2015. 2